

**NEW OBSERVATIONS OF CO ISOTOPOLOGUES TOWARD MASSIVE PROTOSTARS: AN EXPANDED VIEW OF MOLECULAR RESERVOIRS IN THE GALAXY.** Rachel L. Smith<sup>1,2</sup>, Geoffrey A. Blake<sup>3</sup>, A. C. Adwin Boogert<sup>4</sup>, Klaus M. Pontoppidan<sup>5</sup>, Alexandra C. Lockwood<sup>3</sup>, <sup>1</sup>North Carolina Museum of Natural Sciences (rachel.smith@naturalsciences.org), <sup>2</sup>Appalachian State University, Department of Physics and Astronomy, <sup>3</sup>California Institute of Technology, Division of Geological and Planetary Sciences, <sup>4</sup>SOFIA/USRA, NASA Ames, <sup>5</sup>Space Telescope Science Institute.

**Introduction:** High-resolution near-infrared observations of carbon monoxide (CO) gas in absorption have been shown to be powerful tools for the precise derivation of C and O isotope ratios toward solar-type, low-mass protostars within  $\sim 1$  kiloparsec (kpc) of the Sun [1-3]. Results thus far have revealed signatures of CO self shielding – supportive evidence for this process on disk surfaces [2,3,6] – and significant heterogeneity in  $[^{12}\text{CO}]/[^{13}\text{CO}]$ , with possible interplay between CO ice and gas reservoirs as a cause [3-5,6]. Precise ratios of  $[^{12}\text{C}^{18}\text{O}]/[^{12}\text{C}^{17}\text{O}]$  toward low-mass young stellar objects (YSOs) have also been used to argue for supernova enrichment in the early solar system [7], and our recent comparison between low-mass binary systems and embedded protostars suggest carbon isotopic homogeneity within a few hundred AU [6].

As part of our new observational survey of massive YSOs, we present initial results of CO isotopologue abundances toward the highly luminous ( $\sim 7 \times 10^4 L_{\text{Sun}}$ ) protostar AFGL 2136 in the Juggler Nebula,  $\sim 2$  kpc from the Sun and a Galactocentric radius ( $R_{\text{GC}}$ ) of 6.1 kiloparsecs (kpc). We compare these results to other CO reservoirs in this and similar YSOs. Unlike most low-mass objects, bright, massive protostars are observational tracers of regions with high-UV fluxes and several isotopic systems, and span a larger range in  $R_{\text{GC}}$ . Our new  $\text{CO}_{\text{Gas}}$  values provide robust comparisons to solid CO and  $\text{CO}_2$  reservoirs along the same lines of sight, shedding light on key protostellar chemical pathways [8,9].

**Observations and Methods:** Fundamental ( $v = 1 - 0$ ) and first overtone ( $v = 2 - 0$ ) spectra toward five massive protostars were obtained with the NIRSPEC instrument ( $R \sim 25,000$ ) on the Keck II Telescope (Mauna Kea, HI). Spectra were reduced using our customized IDL pipeline; portions of these for AFGL 2136 are shown in Figure 1. The ( $v = 1 - 0$ )  $^{12}\text{C}^{16}\text{O}$  lines are saturated and show complex profiles, so ( $v = 2 - 0$ ) lines are used for analyzing  $^{12}\text{C}^{16}\text{O}$ .

Equivalent widths ( $W_\nu$ ) were determined using a polynomial + Gaussian fit to each isotopologue line (examples in Figure 1). For  $^{12}\text{C}^{18}\text{O}$  and  $^{12}\text{C}^{17}\text{O}$  lines, column densities for each rovibrational line ( $N_J$ ) were calculated directly using the optically-thin relation,  $W_\nu = (\pi e^2 / m_e c^2) f_J N_J$  [10], with  $f_J$  representing the absorption oscillator strength for the  $J^{\text{th}}$  transition. A rotational analysis (Figure 2, top) of the more robust  $^{12}\text{C}^{18}\text{O}$  lines was used to constrain a temperature in

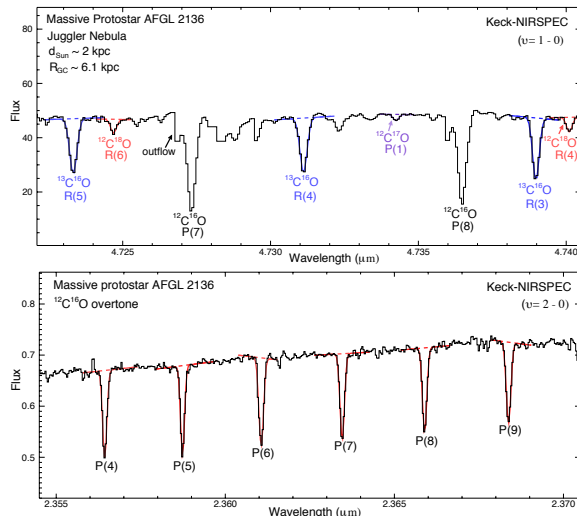


Figure 1: Portions of CO fundamental rovibrational bands toward the massive protostar, AFGL 2136, obtained with Keck-NIRSPEC. Representative CO isotopologue absorption lines are marked. Lines show overlaid model fits, used to derive equivalent widths for each line. (Top): Fundamental band ( $v = 1 - 0$ ) band, where lines for all four CO isotopologues were observed. (Bottom): First overtone ( $v = 2 - 0$ ) band; several  $^{12}\text{C}^{16}\text{O}$  lines are marked.

the curve of growth [10], necessary to find the  $N_J$  for the potentially saturated  $^{12}\text{C}^{16}\text{O}$  and  $^{13}\text{C}^{16}\text{O}$  lines by relating the Doppler line broadening ( $b$ ) to  $W_\nu$ . A preliminary curve of growth using a fixed temperature of 130 K (slightly higher than  $^{12}\text{C}^{18}\text{O}$  following trends found in our earlier data), is shown in Figure 2 (bottom). Total column densities were derived from the rotational analysis (Figure 2 (top), which assumes a Boltzmann distribution for the gas [1-3, 14]).

**Results and discussion:** An initial  $[^{12}\text{CO}]/[^{13}\text{CO}]$  of  $\sim 76 \pm 8$  for AFGL 2136 is plotted against  $R_{\text{GC}}$  of  $\sim 6.1$  kpc (Figure 3). Unlike the dispersion found in our low-mass sources ( $R_{\text{GC}} \sim 8$  kpc), AFGL 2136 follows the predicted Galactic trend for  $[^{12}\text{C}/^{13}\text{C}]$ , consistent with the pattern found in solid  $[^{12}\text{CO}_2]/[^{13}\text{CO}_2]$  toward other massive protostars [8]. Further, the  $[^{12}\text{CO}]/[^{13}\text{CO}]$  of  $\sim 76 \pm 8$  is lower than the solid  $[^{12}\text{CO}_2]/[^{13}\text{CO}_2]$  of  $107 \pm 8$  for this object [8], following the systematic trend suggested for a few other massive protostars [8]. We find a  $[^{12}\text{C}^{16}\text{O}]/[^{12}\text{C}^{18}\text{O}]$  of  $\sim 1700 \pm 180$ , suggesting that CO self shielding may be influencing the oxygen ratios, yet without a robust abundance of  $^{12}\text{C}^{17}\text{O}$  a mass-independent trend cannot be determined. The weak CO ice feature observed

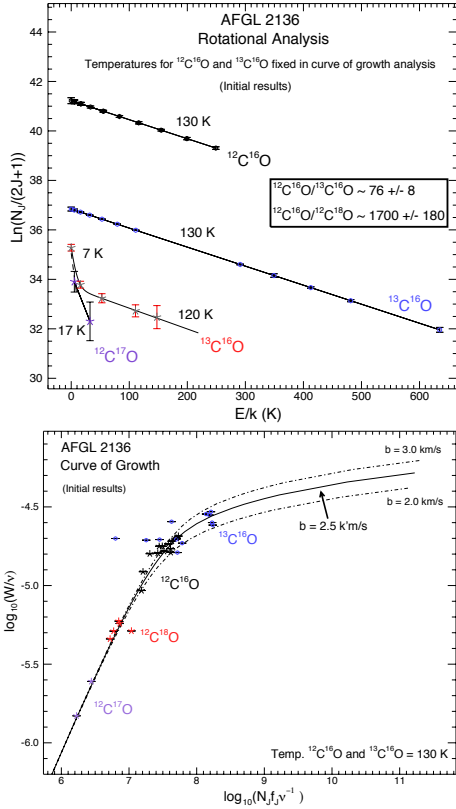


Figure 2: Preliminary analysis for AFGL 2136. (Top): Rotational analysis. Error bars are  $1\sigma$ .  $E_j$  is the energy of the  $J^{\text{th}}$  rotational state, and  $k$  is the Boltzmann constant. (Bottom): Curve of growth showing the  $N_j$  determination for the  $^{12}\text{C}^{16}\text{O}$  and  $^{13}\text{C}^{16}\text{O}$  lines based on a Doppler line broadening ( $b$ ) value of 2.5 km/s and a temperature of 130 K.

in AFGL 2136 [11] further enables comparison of the CO ice fraction vs. the  $^{12}\text{CO}/^{13}\text{CO}$  in the gas (Figure 4). These results so far support the potential observational trend between CO ice and  $^{12}\text{CO}/^{13}\text{CO}$  gas as a possible explanation for the  $^{12}\text{CO}/^{13}\text{CO}$  dispersion seen in our low-mass sample. Continued analysis of our data will help further evaluate these potential trends.

**Conclusions:** Preliminary results for  $^{12}\text{CO}/^{13}\text{CO}$  toward the massive YSO AFGL 2136 suggest that massive protostars may show less carbon isotopic dispersion in distinct molecular reservoirs than found in low-mass objects. Our findings support the possible interplay between CO ice and gas seen in our low-mass sample, as well as the possible real isotopic discrepancy between  $\text{CO}_{\text{Gas}}$  and  $\text{CO}_2(\text{Ice})$  in massive objects. This ongoing survey of massive protostars should help constrain the evaluation of protostellar C and O reservoirs – links to key chemical pathways in these evolving systems.

**References:** [1]Brittain S.D. et al. (2005) *ApJ* 626, 283-291.[2]Smith R.L. et al. (2009) *ApJ* 701, 163-175.[3]Smith

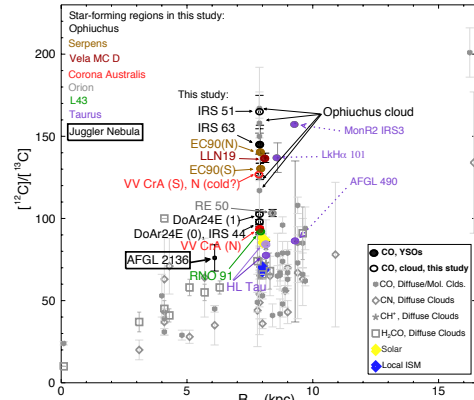


Figure 3: Ratios of  $^{12}\text{C}/^{13}\text{C}$  vs.  $R_{\text{GC}}$  (kpc), including data from the literature and  $\text{CO}_{\text{Gas}}$  from our high-resolution surveys (left labels, filled dots [2,3,6]). AFGL 2136 is boxed at 6.1 kpc. (Top, left): Color-coded molecular clouds associated with each protostar. Values for local ISM ( $\sim 68$  [12]), solar system  $\sim 87$  [13] are shown, with HL Tau from [1] and 3 embedded protostars [14] indicated (purple; right-side labels). Black arrows: diffuse  $^{12}\text{CO}/^{13}\text{CO}$  gas in Ophiuchus [15,16].

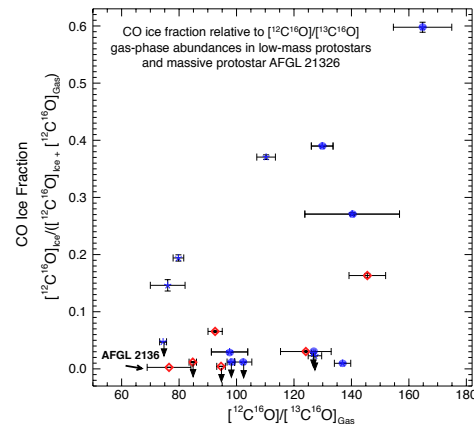


Figure 4: Comparison of the CO ice fraction with  $^{12}\text{C}/^{13}\text{C}_{\text{Gas}}$ . AFGL 2136 value (bottom left) is shown with our low-mass sample [3,6]. Blue stars: cold-gas isotope ratios from regimes where warm gas (red diamonds) was also observed. Blue ovals: objects where *only* cold gas was observed. Total CO ice values were derived from pure CO ice optical depths [11,17]. Arrows:  $3\sigma$  upper limits on ice.

R.L. et al. *ApJ*, submitted.[4] Pontoppidan K.M. (2006) *A&A* 453, L47.[5]Young E.D. and Schauble E.A. *42<sup>nd</sup> LPI*, 1608, 1323.[6] Smith R.L. et al. (2013) *44<sup>th</sup> LPI*, 1719, 2698.[7]Young E.D. et al. (2011) *ApJ*, 729, 43.[8] Boogert A.C.A. et al. (2000) *A&A* 353, 349-362.[9] Boogert A.C.A. et al. (2002) *ApJ* 577, 271-280.[10]Spitzer L. J. (1978) *Physical Processes in the Interstellar Medium*. [16] Pontoppidan K.M. et al. (2003) *A&A* 408, 981-1007.[12] Milam S.N. et al. (2005) *ApJ* 634, 1126-1132.[13] Scott P.C. et al. (2006) *A&A*. 456, 675-688.[14] Goto M. et al. (2003) *ApJ* 598, 1038-1047.[15] Federman S.R. et al. (2003) *ApJ* 591, 989-999.[16] Lambert D.L. et al. (1994) *ApJ* 420, 756-771.[17] Thi W.-F. et al. (2006) *A&A* 449, 251-265.